Investigation of mass transfer phenomena affecting emission rate of gaseous compounds from porous solids

F. Lucernoni[a], L. Capelli[a], V. Busini[a], R. Del Rosso[a], A.A. Prata Jr.[b], R. Stuetz[b], S. Sironi[a]*

[a]Politecnico di Milano, Department of Chemistry, Materials and Chemical Engineering "Giulio Natta" - Piazza L. da Vinci 32, 20133 Milano, Italy
[b]UNSW Water Research Centre, School of Civil and Environmental Engineering, The University of New South Wales, Sydney, NSW, 2052, Australia

*Corresponding author, e-mail selena.sironi@polimi.it

Abstract

Emissions of atmospheric pollutants from facilities like wastewater treatment plants or landfills typically come from so called "passive area sources". Such emissions, often resulting in direct or indirect health effects on the population, are hardly quantifiable, because of the lack of standardization regarding sampling and assessment from this kind of source.

Passive solid area sources are most commonly sampled using specific enclosure devices (hoods). However, fluxed hoods with different designs and different operating conditions produce results that are not comparable to each other.

In this work, two mathematical models for the description of the mass transfer inside a wind tunnel were compared with experimental data in order to define the actual fluid dynamics in different configurations. The tests involved first a liquid source and then a solid bed, using different airflow rates and different bed thicknesses. Results showed that the behaviour of emissions from solid porous media are affected by the sweeping airflow rate, but the dependency is different to the case of liquid sources. For solids with limited porosity intra-phase diffusion becomes the controlling stage for diffusion, thus giving that the emission rate becomes constant with respect to the sweeping airflow rate.
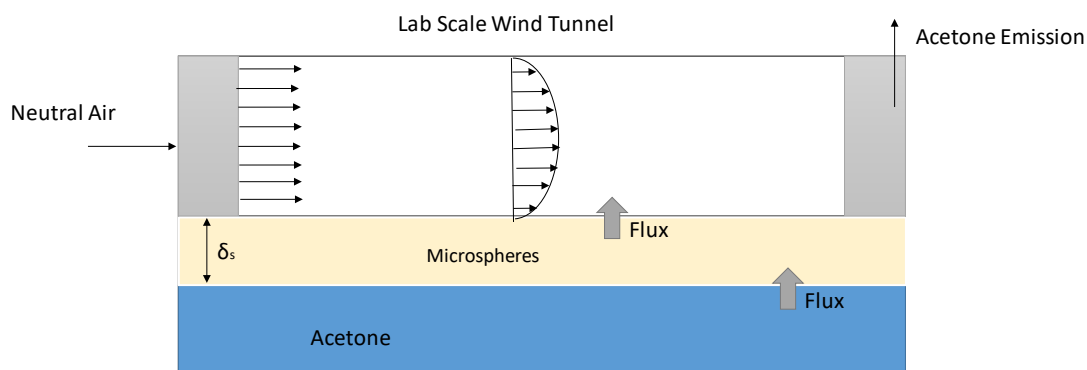
Keywords

Gaseous emissions, liquid area sources, solid area sources, odorants, hood sampling, wind tunnel

Highlights

- Different hoods currently used for sampling on passive area sources produce results that are not consistent nor comparable
- Mass transfer phenomena occurring inside the hood are not fully understood.
- A new method is proposed to evaluate emissions of gaseous pollutants from solids.
- Emissions from porous media are proven to be affected by airflow rate.
- Mass transfer and its dependency on the ventilation rate is different to the case of liquid surfaces.

Graphical Abstract

1. Introduction

Atmospheric emissions from facilities such as wastewater treatment and waste management plants, agricultural operations and landfills, if not directly hazardous, often lead to nuisance and complaints in the neighbouring areas (Guo et al., 2003; Hayes et al., 2014). In such plants, gaseous pollutant emissions typically come from so called "passive area sources" and are typically produced by the aerobic and anaerobic processes that occur into the liquid or solid mass, either directly from the microorganisms or as a consequence of chemical-physical interactions between compounds (Gostelow et al., 2001). Such emissions usually are a complex mixture many different compounds, either volatile organic compounds (VOCs) such as acetone and benzene or non-VOCs such as ammonia, hydrogen sulfide and other reduced sulfur compounds (Cai et al., 2007). Most of the gaseous pollutants emitted may not represent a direct hazard for human health, but they are often characterized by low odour detection threshold, thereby causing odour nuisance in the near-living population, which may result in adverse health effects (Aatamila et al., 2011).

A range of different direct assessment approaches has been applied to the evaluation of gaseous emissions from passive area sources, typically known as enclosure device techniques (i.e. hood methods). Such methods entail the use of some sort of chamber that is capable of isolating a sub-area of the emissive surface (Bahlman et al., 2006; Dai and Blanes-Vidal, 2013; Zhang et al., 2016; Song et al., 2008; Dunlop et al., 2016). These chambers can be either passive (i.e. static hoods) or dynamic. Dynamic hoods, differ from static chambers in that these systems require a neutral flushing gas to sweep the surface; these devices can be with directional flow (wind tunnels (WT)) or non-directional flow (flux chambers) and, independently from the design and volume of the chambers, are operated with large flow rates (i.e. high speed) or small flow rates (i.e. low speed).

There are challenges and technical limitations with enclosure sampling as different designs typically produce results that are not consistent and are not comparable to those obtained with different chambers. This uncertainty is often the result of limited benchmarking of the mass transfer phenomena taking place inside such devices as well as the tools used to assess the

emission devices themselves. More detailed examples of the variety of possible designs (Leyris et al., 2005; Kolari et al., 2012; Catalan et al., 2009; Galvin et al., 2004; Taha et al., 2005; Bliss et al., 1995; Van Belois & Anzion, 1992; Park & Shin, 2001; Parker et al., 2010; Parker et al., 2013; Prata Jr. et al., 2016; Santos et al., 2012) are shown in Supplementary material (Table A1).

The study of gas and odorant emissions from different solid porous media (such as wastewater sludge, poultry litter and contaminated soils) is an important task that has not been fully investigated (Capelli et al., 2013). This is especially the case for solid materials that present a deeper level permeated with an evaporating volatile liquid and/or a dried-out upper level in contact with the atmosphere. For emissions from porous solids, the mass transfer phenomenon can be generally described by Thibodeaux (1996): diffusion in the liquid phase, volatilisation, diffusion through the solid's pores to the surface, migration of the odorant to the overlying gas phase, diffusion to the gaseous bulk and following advection due to the wind action on the solid surface.

There are several studies addressing the correlation of emission rate with the sweep air velocity, both for the case of solid sources (Capelli et al., 2012; Zhang et al., 2002; Nakano et al., 2004) and liquid sources (Hudson and Ayoko, 2008; Thibodeaux and Scott, 1985; Capelli et al., 2009), for inside the sampling hood (Hudson and Ayoko, 2008; Nakano et al., 2004) and open field situations (Kawamura and McKay, 1987; Fingas, 1998). For example, Capelli et al. (2009) studied the phenomenon inside a sampling WT device and validated a model using Eq. (1)-(3), relying on Prandtl's Boundary Layer Theory for forced convection over a flat plate (Thibodeaux and Scott, 1985):

$$ER = SER * A_{em} = \frac{Q_{air} * c_i}{A_b} * A_{em} \qquad (1)$$

$$c_i \propto v^{-\frac{1}{2}} \qquad (2)$$

$$ER \propto Q_{air} * c_i \propto v * A_i * v^{-\frac{1}{2}} \propto v^{\frac{1}{2}} \qquad (3)$$

Where: (ER) Emission Rate [ou/s or mg/s], (SER) Specific Emission Rate [ou/m^{2}s or mg/m^{2}s], (A_{em}) emissive area [m^2], (Q_{air}) fluxed neutral air flow rate [m^3/s], (c_i) compound concentration in the hood outlet steam [ou/m^3 or mg/m^3], (A_b) WT base area [m^2], (v) air speed [m/s],, (A_i) WT cross section area [m^2].
For further clarification SER is the quantity of substance emitted per unit of surface and time, emissive area is the area of the source (for example the area of a tank or a heap), whereas the base area is the base area of the wind tunnel, which typically covers a small part of the emissive area. The air speed is the speed of the sweeping airflow inside the hood calculated as the ratio between sweeping air flow rate [m^3/s] and hood cross section [m^2].

Eq. (3) assumes that the motion regime is laminar. Laminar flow is the most common condition inside sampling hoods, although it should be considered that the effective air flow on real sources (e.g., wastewater treatment tanks of big dimensions) is mostly turbulent, giving that suitable models will be necessary in order to extend wind tunnel considerations to real field conditions (Lucernoni et al., 2017) While the model of Eq. (3) seems to work fine for the liquid, its application for a solid surface scenario is more complex and a more suitable specific volatilisation model is necessary (Capelli et al., 2013), which builds on previous emission research from area sources (Thibodeaux, 1996; Zhang et al., 2002).

This study aims to develop a more appropriate methodology to evaluate the dependency of emission rate (ER) (or equivalently the concentration in the gas phase) on the diffusivity through the solid porous medium and on the air flow motion regime. The research investigated the issue of emissions from solid area sources on the basis of a laboratory-scale system that simulates a real situation, (i.e. a surface emission of a gas generated in the deeper wet levels). A specific wind tunnel device was used simulate the phenomenon at different stages of complexity, both in static and dynamic conditions and a comprehensive model was applied to describe the phenomenon, which was capable of predicting the emissive flow and the resulting gas concentration in the gas phase.
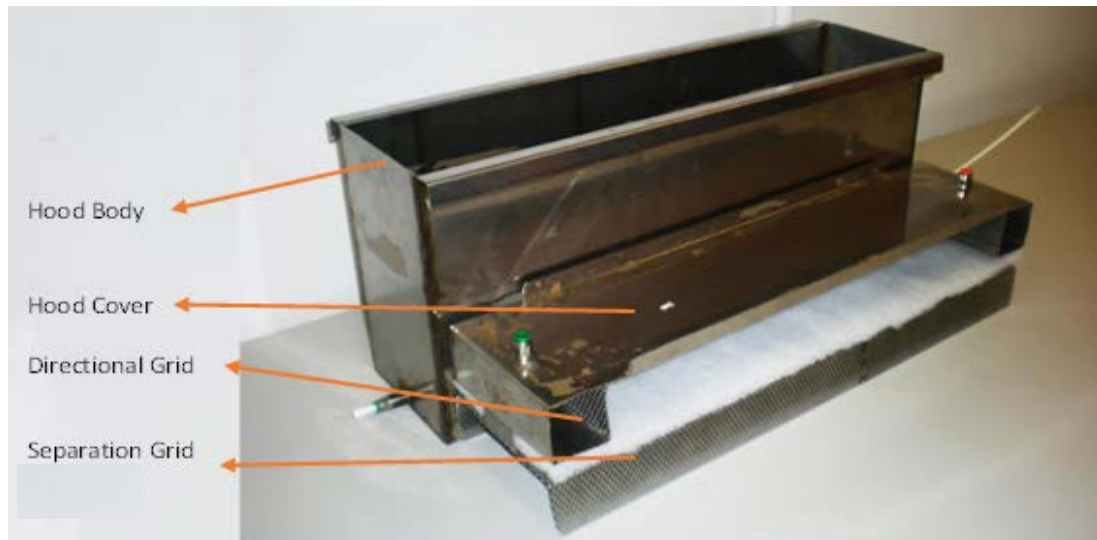
2. Materials and Methods

A WT sampling device was used in laboratory-scale experiments to assess the concentration of acetone (chosen as a reference gas representative of the components typically found in contaminated soils, aerobic solid waste treatment plants, wastewater treatment plant sludges) being emitted from a simulated solid surface. The phenomenon reproduced is treated with an increasing degree of complexity: a simple liquid-gas bi-phase system is considered first and then microspheres are introduced, thus obtaining a solid bed with a dry layer crossed by a diffusive flow of acetone originated in the lower levels wetted by the liquid acetone. The dry layer width was changed over different trials. At all stages both static and dynamic tests were performed, thereby changing the sweep air flow rate in order to investigate the dependence on the air speed.
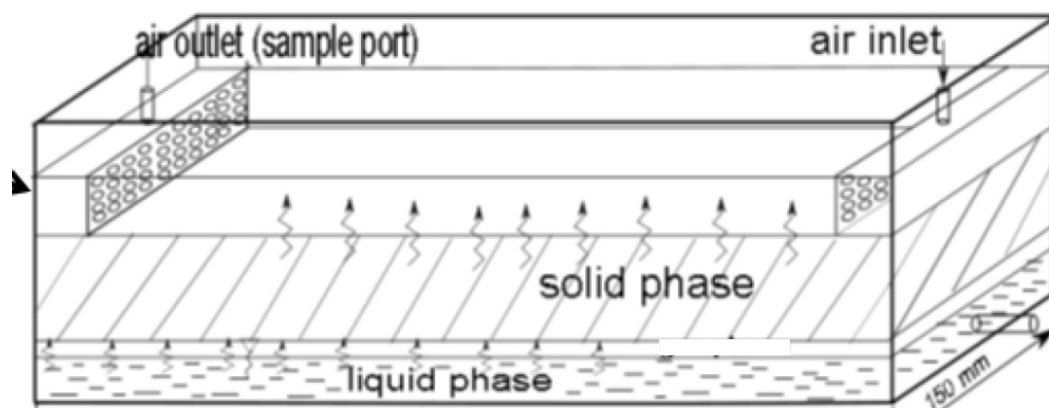
2.1 Experimental Setup

In order to simulate a typical situation that can be investigated analytically, the air flow inside the wind tunnel needs to be uniform and fully developed; this is why a proper design of the hood is necessary: for homogeneity vertical velocity gradients should be avoided, e.g., by limiting the height of the WT as suggested by several authors (Loubet *et al.*, 1999; Sohn *et al.*, 2005). For a fully developed flow it is crucial to guarantee a hood length of at least equal to 3 times the equivalent diameter from the entrance zone (Bird-Stewart-Lightfoot, 2002). The designed wind tunnel satisfied this requirement.

The WT device was made of stainless steel, a material that does not interfere with the fluids involved in the experiments, i.e. water, air, acetone (CEN EN 13725, 2003). The WT has a rectangular base and a rectangular cross-section (dimensions: length, 60 cm x height, 20 cm high x width, 15 cm). The top of the wind tunnel had a removable cover that can be adjusted at different heights, allowing to regulate the free head-space in the hood and to easily clean the device. The cover is also equipped with inlet and outlet orifices on the top wall and two grates 5 cm high with 6 mm diameter holes – opened only on the face with dimensions 5 cm x 15 cm – that assure a directional gas flow parallel to the surface under evaluation (i.e. no vertical mixing); the grid was placed exactly on top of the emitting surface to avoid deviations in the streamlines. The designed wind tunnel (Fig. 1 and Fig. 2) satisfies all the above mentioned requirements.

Figure 1. *The Wind Tunnel device.*

Figure 2. *The Wind Tunnel scheme.*

The experimental study simulated the emitting solid as a layer without discontinuities, having the deeper levels wet with the liquid acetone and the upper levels dry.

The solid layer was made of glass microspheres with diameters ranging from 400 μm to 800 μm; glass was chosen as it is inert and odourless, and microspheres in order to have a good porosity. The characteristics of the bed are: void fraction 37.3% and tortuosity 2.083.

Figure 3. *The glass microspheres.*

The void fraction was evaluated empirically measuring a known solid volume and the liquid volume that was possible to add to the packed bed without varying the level of the solid; for the tortuosity the default Blake-Kozeny value (Kozicki and Tiu, 1988) was adopted, acceptable for a wide range of solid beds.

Acetone (C_3H_6O) was selected for the experimental study's due to its, volatility, non-boiling liquid characteristics, low odour detection threshold, and is easily detectable via gas chromatograph. Moreover, acetone is a good reference compound (see Appendix A) as it is representative of the components that are typically found in contaminated soils, in the emissions from aerobic solid waste treatment plants (Zhang *et al.*, 2012; Fricke *et al.*, 2005) as well as wastewater treatment plants sludge (Wu *et al.*, 2006). The TLV-TWA level for acetone is 750 ppm, thus acetone was deemed safe enough to be used for the experiments.

2.2 Experimental methods

The experiments were carried out at different flow situations, i.e. setting different flow rate values for the forced neutral air flux sent into the wind tunnel in order to simulate the wind action over the solid surface: no flow (static condition), minimal flow (0.65 m³/h), medium flow (1.25 m³/h) and high flow (2.40 m³/h). The flushed runs last for a period of 3 min. The air flow is provided through a compressor feeding a Teflon® pipe linked to the WT 6 mm diameter inlet, where the flow is stabilises due to a diffusion grid. The flow rate is adjusted using a rotameter and a regulation valve. The following tests were performed:

- liquid only (no solid/glass microspheres); static hood plus three different air speeds;
- dry solid, a 1 cm dry solid layer above the wet layer (3 cm imbued with liquid acetone); static hood plus three air speeds;
- dry solid, a 2 cm dry solid layer above the wet layer; static hood plus three air speeds;
- dry solid, a 5 cm dry solid layer above the wet layer; static hood plus three air speeds;
- dry solid, a 8 cm dry solid layer above the wet layer; static hood plus three air speeds.

The sampling at the outlet of the wind tunnel were collected by means of a gas syringe, with 0.1 mL being injected into a Gas Chromatograph coupled to a Thermal Conductivity Detector (GC-TCD) (HP6890, USA). The GC-TCD analysis conditions included using a general purpose column (Supelco, USA) with a fused silica filling (30 m long, inner diameter 0.53 mm, film thickness 0.50 μm), a flow rate of 2.0 ml/min with helium as the carrier gas at an oven temperature of 30°C. This provided an analysis time of 10 minutes, which enabled experiments to be repeated many times and acetone concentrations to be expressed in ppm.

2.3 Diffusion and volatilization models

An important aspect to consider is that it is necessary to distinguish between the situation inside a sampling wind tunnel and the situation in the open field. For the situation in the open field, it possible to rely on several studies that provided satisfactory expressions giving the emission rate from area sources. The fundamental theory for these kind of problems was provided by Sutton (1934), who devised the expression here reported:
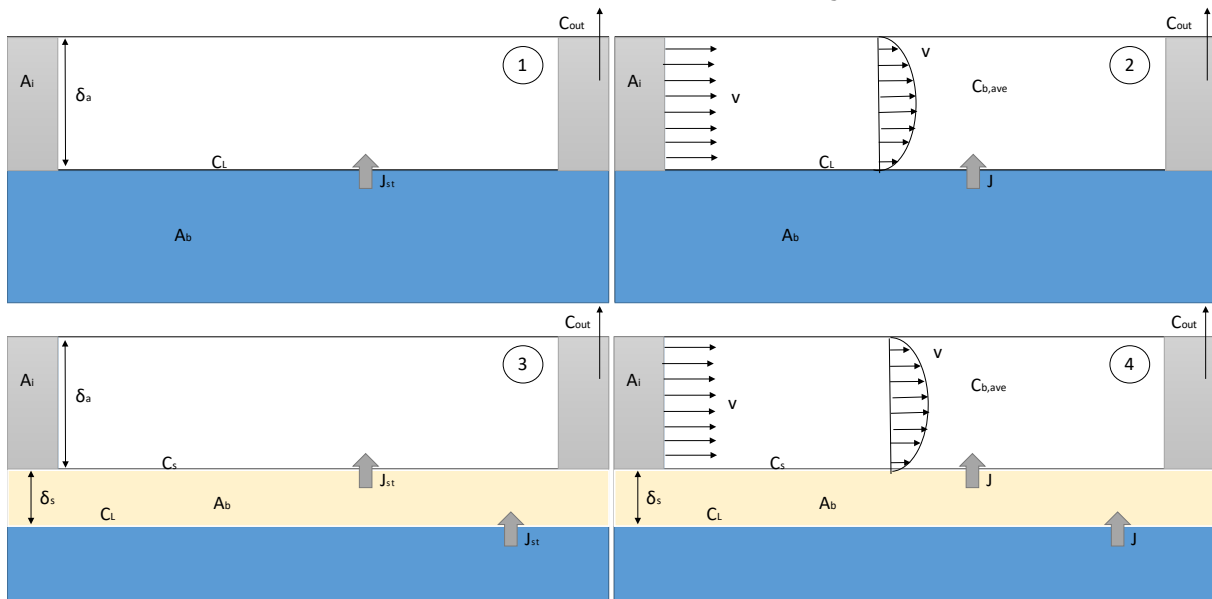
$$E = K \, u^{\frac{2-n}{2+n}} \, a^{\frac{2}{2+n}} \, x_0^{-\frac{n}{2+n}}$$

(4)

Where: (E) is the emission rate, (u) is the wind velocity measured at a given height (i.e., the height at which anemometers data are available), (a) is a parameter depending on the atmospheric characteristics of the area, (x_0) is the leeward source length, (n) is a parameter function of the wind velocity profile on the pool surface which for a neutral stability class can be assumed constant and equal to 0.25, (K) is a proportionality coefficient. Based on Sutton's dissertation, several later studies have been able to determine semi-empirically the constant terms (K) and (a) (Kawamura and MacKay, 1987; MacKay and Matsugu, 1973; Yellow Book, 1992), whose values are usually what distinguish one model from the other. For further details, a recent publication discusses the application of one of these models for the extensions of wind tunnel results to the evaluation of open field emissions of some odorants (Lucernoni et al., 2017).

For the situation inside the sampling wind tunnel, the fluid-dynamics is different and the formulation of models, capable of describing the dependency of emission on different parameters varying into the hood, is the aim of this work. The task will be achieved comparing two suitable mathematical models of the mass transfer in the wind tunnel with experimental results to define which one describe better the actual phenomena. Thus, in this section, the suggested models are presented following the same scheme as the experiments:

1. static hood (i.e. flush rate zero) with evaporating liquid;
2. fluxed chamber with evaporating liquid;
3. static hood (i.e. flush rate zero) with emission from a dry porous solid above a wet solid layer;
4. fluxed chamber with emission from a dry porous solid above a wet solid layer;

Four experimental setups are schematised in Fig. 3, in which: (v) is the horizontal air velocity inside the wind tunnel, (A_i) is the inlet/outlet cross section i.e. the grid area, (δ_a) is the distance crossed by the flux (i.e. 5 cm, the chamber's height), (A_b) is the liquid bed area, (J_{st}) is the emissive flow for the static scenario, (J) is the emissive flow for the fluxed situation, (C_L) is the equilibrium concentration above the liquid surface, ($C_{b,ave}$) is the average effective bulk concentration in the gas phase, (C_{out}) is the outlet concentration in the gas phase, (C_S) is the concentration into the gas phase at the gas-solid interface, (δ_s) is the dry bed thickness.

Figure 4. *Scheme of gaseous emission from a liquid surface (1 and 2) and from a solid surface (3 and 4).*

In Fig. 4 it is possible to see the flat velocity profile at the inlet, which develops in the parabolic profile for laminar flows.

For the static situation of evaporating liquid, it is possible to adopt the analogy with the diffusion through a stagnant film as reported by Mauri (2011), obtaining the expression for the flux (J_{st}) here reported:

$$J_{st} = \frac{\wp_{mol,ACE} * C_{tot}}{\delta_a} * LN\left(\frac{1 - \frac{c_{b,\delta_A}}{C_{tot}}}{1 - \frac{C_L}{C_{tot}}}\right) \tag{5}$$

Where: ($\wp_{mol,ACE}$) is the molar diffusivity of the evaporated vapor (i.e. acetone) in air, (c_{b,δ_A}) is the bulk concentration of acetone at the top of the chamber in the gas phase, (C_{tot}) is the total concentration in the chamber (i.e. $\frac{P_{tot}}{RT}$), (P_{tot}) is the total pressure inside the chamber, (C_L) is the equilibrium concentration (i.e. the concentration obtained at the vapor pressure at temperature T, $P^0(T)$, as $\frac{P^0(T)}{RT}$).

At this point, by means of a mass balance it is possible to evaluate the concentration trend over time and compute the value at a given time:

$$\frac{dC_{b,\delta_A}}{LN\left(\frac{1 - \frac{c_{b,\delta_A}}{C_{tot}}}{1 - \frac{C_L}{C_{tot}}}\right)} = \frac{\wp_{mol,ACE} * C_{tot}}{\delta_a} * \frac{A_b}{V} * dt \tag{6}$$

This ordinary differential equation can be solved numerically. This also allows determination of the time required for the concentration to become constant in the wind tunnel. That is the time when the fluxed run can be started.

For the situation of an emitting liquid surface in presence of an air flux (Thibodeaux and Scott, 1985; Capelli et al., 2009), Eq. (7) holds true:

$$C_{out} = a * v^{-\frac{1}{2}} \tag{7}$$

Where: (C_{out}) is the concentration at the outlet and (a) is a proportionality constant. Such dependence from the velocity can be explained starting from the stationary mass balance inside the chamber:

$$Q_{air}^{in} \cdot C_{in} + J \cdot A_b = Q_{air}^{out} \cdot C_{out} \tag{8}$$

Assuming that the concentration of the contaminant in the fluxed air (C_{in}) is zero and that $J \ll Q_{air}^{in}$, it is possible to consider $Q_{air}^{in} \sim Q_{air}^{out} = Q_{air}$ and write the concentration at the outlet (C_{out}) as the ratio between the emission and the sweep air flow rate as shown in Eq. (9):

$$C_{out} = \frac{J * A_b}{Q_{air}} = \frac{k_C * (C_L - C_{b,ave}) * A_b}{v * A_i} = a * v^{-\frac{1}{2}} \tag{9}$$

With:

$$C_L = \frac{PM * P_0(T)}{R * T} \tag{10}$$

Where: (PM) is the molecular mass of the compound.

Now, considering that the section of the WT is a wide and short rectangle, it is possible to suppose that the mass transfer from the emitting liquid surface is like the one known for a flat plate ((Bird, Stewart, Lightfoot, 2002) and to write the mass transfer coefficient (k_C) as:

$$k_C = \left(\frac{\wp_{mol,ACE}}{L_{WT}}\right) * \left(0.664 * Re^{\frac{1}{2}} * Sc^{\frac{1}{3}}\right) = \left(\frac{\wp_{mol,ACE}}{L_{WT}}\right) * \left(0.664 * \left(\frac{v*L_{WT}}{v_{AIR}}\right)^{\frac{1}{2}} * \left(\frac{v_{AIR}}{\wp_{mol,ACE}}\right)^{\frac{1}{3}}\right) \quad (11)$$

Where: ($\wp_{mol,ACE}$) is the diffusivity coefficient for acetone, (L_{WT}) is the WT length, (Re) is the Reynolds number, (Sc) is the Schmidt number, (v) is the air speed in the wind tunnel, (v_{AIR}) is the air kinematic viscosity. Hence, equaling the two expressions for C_{out}, the dependency on the velocity is explicit:

$$C_{out} = \frac{k_C*(C_L-C_{b,ave})*A_b}{v*A_i} = \frac{k_C*C_L*A_b}{v*A_i+0.5*k_C*A_b} = f\left(v^{-\frac{1}{2}}\right) \quad (12)$$

In Eq. (12) the average concentration inside the chamber ($C_{b,ave}$) is assumed equal to the 50% of the concentration at the outlet.

Another possible expression for the mass transfer coefficient, involves the analogy with heat/mass transfer phenomena for internal flows between parallel flat plates (Bird, Stewart, Lightfoot, 2002; Perry, 1997; Incropera, DeWitt, Bergman, Lavine, 2007; Shah and London, 1978). These authors all refer to the case of heat transfer, but the results can be extended to mass transfer problems by means of the Colburn's analogy.

The delicate point is the evaluation of the mass transfer coefficient:

$$k_c = \frac{Sh*\wp_{mol,ACE}}{D_e} \quad (13)$$

$$Sh = Nu * \left(\frac{Sc}{Pr}\right)^{1/3} \quad (14)$$

$$Sc = \frac{v_{AIR}}{\wp_{mol,ACE}} \quad (15)$$

$$Pr = \frac{v_{AIR}}{\alpha_{ACE}} \quad (16)$$

$$Nu = 4.425 * \left(\frac{\left(\delta_a/2\right)^{2/3}}{\alpha_{ACE}^{1/3}*L^{1/3}}\right) * v_{air}^{1/3} \quad (17)$$

$$k_c = \left(\frac{\wp_{mol,ACE}}{D_e}\right) * \left(Nu * \left(\frac{Sc}{Pr}\right)^{1/3}\right) = \left(\frac{\wp_{mol,ACE}}{2*\delta_a}\right) * \left(4.425 * \left(\frac{\left(\delta_a/2\right)^2 *v_{air}}{L*\alpha_{ACE}}\right)^{1/3} * \left(\frac{\alpha_{ACE}}{\wp_{mol,ACE}}\right)^{1/3}\right) \quad (18)$$

Where in Eq. (13)-(18) the Colburn's analogy was applied and (Sh) is the Sherwood number, (D_e) is an equivalent diameter (for this case, $2 * \delta_a$), (Nu) is the Nusselt number, (Sc) is the Schmidt number, (Pr) is the Prandtl number, (v_{AIR}) is the kinematic viscosity of air, (α_{ACE}) is the thermal diffusivity of acetone, (L) is the plates length (i.e. the WT length L_{WT}), (v_{air}) is the air velocity (inside the WT).

Therefore, considering also in this case ($C_{b,ave}$) equal to the 50% of the concentration at the outlet:

$$C_{out} = \frac{k_C*(C_L-C_{b,ave})*A_b}{v*A_i} = \frac{k_C*C_L*A_b}{v*A_i+0.5*k_C*A_b} = f\left(v^{-\frac{2}{3}}\right) \quad (19)$$

In the following sections, it will be discussed whether the single flat plate or the parallel flat plates expression is better for the evaluation of the mass transfer coefficient.

The previous dissertation allows moving to the more complex situation involving a solid porous layer; the situation schematized in Fig. 3, bottom, box 3 and box 4.

For the case of static hood, in analogy with what was described with Eq. (5)-(6), it is possible to write an ordinary differential equations system (ODES) and the interface concentration (c_s) can be directly determined:

$$\begin{cases} \dfrac{dc_S}{dt} = \dfrac{A_b}{V_s} * \dfrac{\wp_{eff,ACE}}{\delta_S} * c_{tot} * \ln\left(\dfrac{1-\frac{C_S}{C_{tot}}}{1-\frac{C_L}{C_{tot}}}\right) \\[3ex] \dfrac{dc_{b,ave}}{dt} = \dfrac{A_b}{V_a} * \dfrac{\wp_{mol,ACE}}{\delta_a} * c_{tot} * \ln\left(\dfrac{1-\frac{C_{b,ave}}{C_{tot}}}{1-\frac{C_S}{C_{tot}}}\right) \end{cases} \qquad (20, 21)$$

Where (V_s) is the volume of the solid, (V_a) is the volume of the air in the chamber, ($\wp_{eff,ACE}$) is the effective diffusivity of acetone in air, (δ_S) is the distance crossed by the flux in the solid (i.e. 1/2/5/8 cm), (c_s) is the concentration at the gas-solid interface, ($c_{b,ave}$) is the mean concentration in the hood.

The resolution provides the stationary value of (c_s) and ($c_{b,ave}$) at any given time.

Finally, for the situation of the fluxed hood, it is possible to write an equation expressing that (J) is continuous, formulaically:

$$J = k_C * \left(C_S - C_{b,ave}\right) = \frac{\wp_{eff,ACE}}{\delta_S} * (C_L - C_S) \qquad (22)$$

Where: (k_C) is the mass transfer coefficient, ($\wp_{eff,ACE}$) is the effective diffusivity of acetone through the porous layer, equal to the molecular diffusivity in air multiplied by the porosity (ε) and divided by the tortuosity (τ) of the medium, and (δ_S) is the dry layer thickness.

Eq. (22) allows the expression to be written for the concentration at the solid-gas interface (Cs) as shown in Eq. (23)-(24):

$$(k_C * C_S) - (k_C * C_{b,ave}) - \left(\frac{\wp_{eff,ACE}}{\delta_S} * C_L\right) + \left(\frac{\wp_{eff,ACE}}{\delta_S} * C_S\right) = 0 \qquad (23)$$

$$C_S = \frac{(k_C * c_{b,ave}) + \left(\frac{\wp_{eff,ACE}}{\delta_S} * C_L\right)}{\left(k_C + \frac{\wp_{eff,ACE}}{\delta_S}\right)} \qquad (24)$$

Knowing (C_S) enables to investigate the dependency of the outlet concentration (C_{out}) on the air speed, as shown in Eq. (25):

$$C_{out} = \frac{A_b * J}{A_i * v} = \frac{A_b * k_C * (C_S - c_{b,ave})}{A_i * v} \qquad (25)$$

Through further rearrangements of Eq. (25), that is substituting the expression of C_s and by considering also in this case ($C_{b,ave}$) equal to the 50% of the concentration at the outlet, it is possible to write:

$$C_{out} = \frac{A_b * \frac{\wp_{eff,ACE}}{\delta_S} * k_C * C_L}{A_i * v * \left(k_C + \frac{\wp_{eff,ACE}}{\delta_S}\right) + 0.5 * A_b * \frac{\wp_{eff,ACE}}{\delta_S} * k_C} \qquad (26)$$

Eq. (26) allows to make some interesting considerations:

- For (k_C) $\gg$ ($\frac{\wp_{eff,ACE}}{\delta_S}$), i.e. high values of ($v$) and/or high values of (δ_S), (C_{out}) will be proportional to the speed (v) to an exponent of (-1);

- For (k_C) $\ll$ ($\frac{\wp_{eff,ACE}}{\delta_S}$), i.e. low values of ($v$) and/or minimal values of (δ_S), (C_{out}) will be proportional to the speed (v) to an exponent of (-0.5) or (-0.67), thus resembling the "liquid only" case, depending on the model chosen (flat plate or parallel plates).

In analogy with Eq. (7), it s possible to write Eq. (27) for the case of a solid area source:

$$C_{out} = a' * v^{\alpha} \qquad (27)$$

The experimental results reported in the next section were used to determine the exponent: that is the situations in which the limiting phenomenon is the diffusion through the porous solid or the mass transfer in the wind tunnel and to discriminate between the parallel flat plates or flat plate model for mass transfer coefficient.

3. Results and Discussion

Before each fluxed run, a "static" experiment (no flow) was performed in order to check that the initial working condition were the same (i.e. at the equilibrium condition). For each situation the concentration expression was solved by means of a Matlab® code, Eq. (6) for the liquid or Eq. (19, 20) for the solid, in order to determine the time to await in order to reach the steady- state condition. In the case of the solid this procedure also provided the interface concentration required to compute the outlet concentration for the fluxed runs. In that regard, it was concluded that this was the most suitable model to describe the situation inside the chamber during the static period.

For the sake of clarity, Tab. 1 reports the value of the parameters used for the theoretical computations.

Table 1. *Parameters for the theoretical computations.*

PM	5.80E-02	kg/mol
,mol,ACE	1.06E-05	m2/s
,eff,ACE	1.90E-06	m2/s
A,a	4.42E+00	-
B,a	1.31E+03	-
C,a	-3.24E+01	-
A,i	7.50E-03	m2
A,b	7.50E-02	m2
ν,AIR	1.51E-05	m2/s
ε	0.373	-
τ	2.083	-

In Tab. 1 are reported, in order: acetone molecular weight, acetone molecular diffusivity in air, acetone effective diffusivity in air, (A,a) Antoine's equation parameter for acetone, (B,a) Antoine's equation parameter for acetone, (C,a) Antoine's equation parameter for acetone (http://webbook.nist.gov/chemistry), the wind tunnel cross section area, the hood base area, the kinematic viscosity of air, the porosity of the packed bed, the tortuosity of the packed bed.
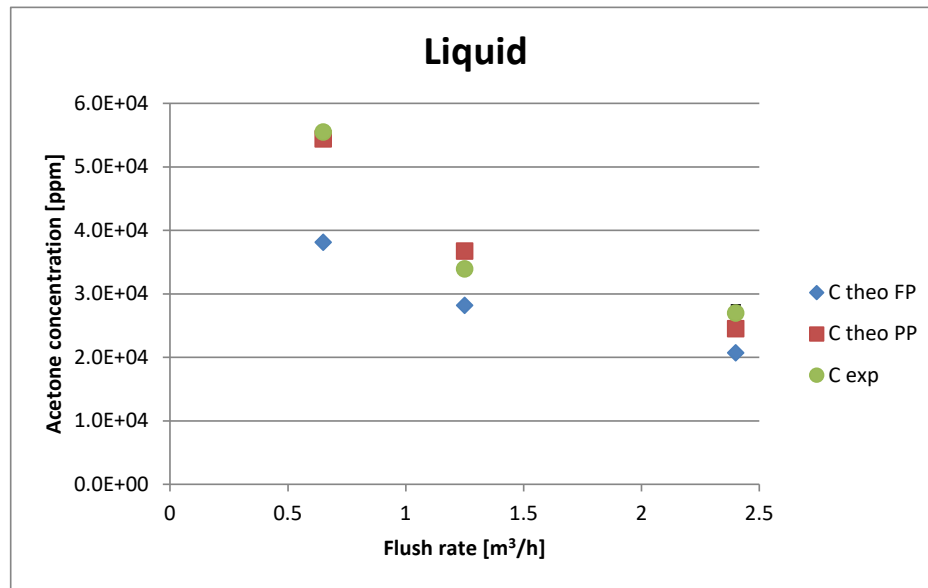
3.1 The liquid case

First the static test was performed. The experimental value obtained after 20 min, at the stationary condition, was 226'000 ppm while the theoretical calculated value was 222'000 ppm, computed in Matlab® by solving Eq. (6); the agreement is satisfactory.

Moving to the flushed case, the results of the tests are depicted in Tab. 2 and in Fig. 4: in Tab. 2 the third column refers to the theoretical values computed for the flat plate (FP) model (Eq. 12) while the fourth column refers to the values computed for the parallel plates (PP) model (Eq. 18). The same acronyms are used also in the following figures and tables.

Table 2. *Mean concentrations for the "liquid only" case.*

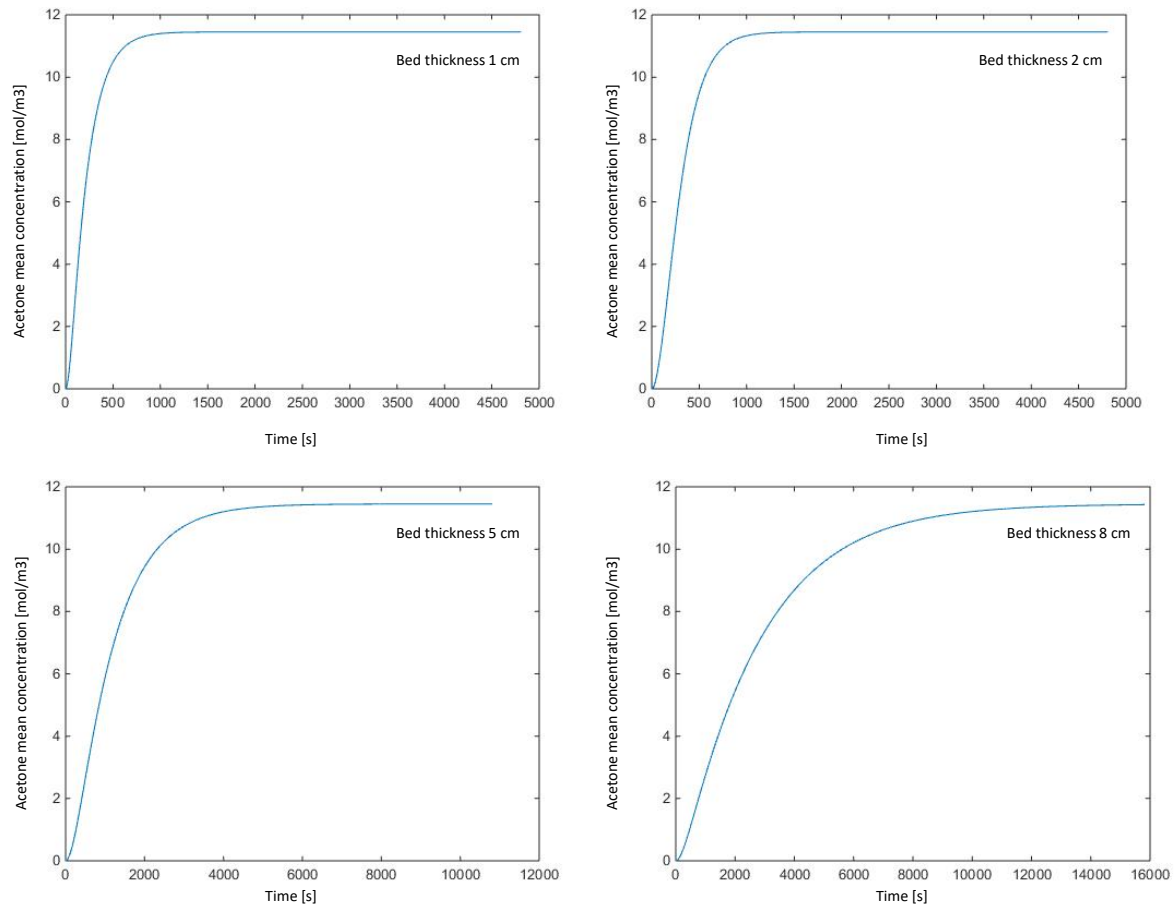| Air flow rate [m3/h]	C exp [ppm]	C theo FP [ppm]	C theo PP [ppm]
0.65	55000	38000	54000
1.25	34000	28000	37000
2.4	27000	21000	24000

Figure 5. *Comparison of theoretical and experimental mean concentrations, "liquid only".*

Experimental errors are so contained that the errors bars are not visible in the figure.

It is possible to see that also in the fluxed runs, performed flushing different air-flow rates inside the wind tunnel, it was found a rather good agreement between theory and experiments, especially for the intermediate and high flush rates.

3.2 The solid case

Since the gas-solid interface concentrations are required for the computation of the outlet concentrations for the flux cases, and both room and pool temperature were found to vary from one experiment to the other. They were evaluated according to Eq. (20, 21) for the four different scenarios (i.e. bed thicknesses of 1/2/5/8 cm) at the actual temperature of the liquid acetone measured at the beginning of each experiment. The (C_s) values refer to the concentration at the time when the fluxed runs were started. Particularly for the experiments at thicknesses of 5 cm and 8 cm, the time required to reach the actual stationary value for the average concentration inside the chamber is great (from 2 to 4 h) but the time to reach a value very similar to the stationary is much less (i.e. growth rate very slow in the period preceding the stationary, after 1 h), therefore it was decided to start the flushed runs after this time for logistical reasons. The times awaited before the fluxed runs were started are: 22 min for the 1 cm bed thickness, 30 min for the 2 cm bed thickness, 60 min for the 5 cm bed thickness, 60 min for the 8 cm bed thickness. An example for the mean acetone concentration trend over time inside the wind tunnel is shown in Fig. 6, evaluated at 21°C for the different bed thickness values by means of a Matlab® code.

Figure 6 *Computed mean acetone concentration trends over time.*

In analogy with the liquid case, the theoretical and experimental static concentrations were compared, as shown in Tab. 3, which reports acetone temperature as well.
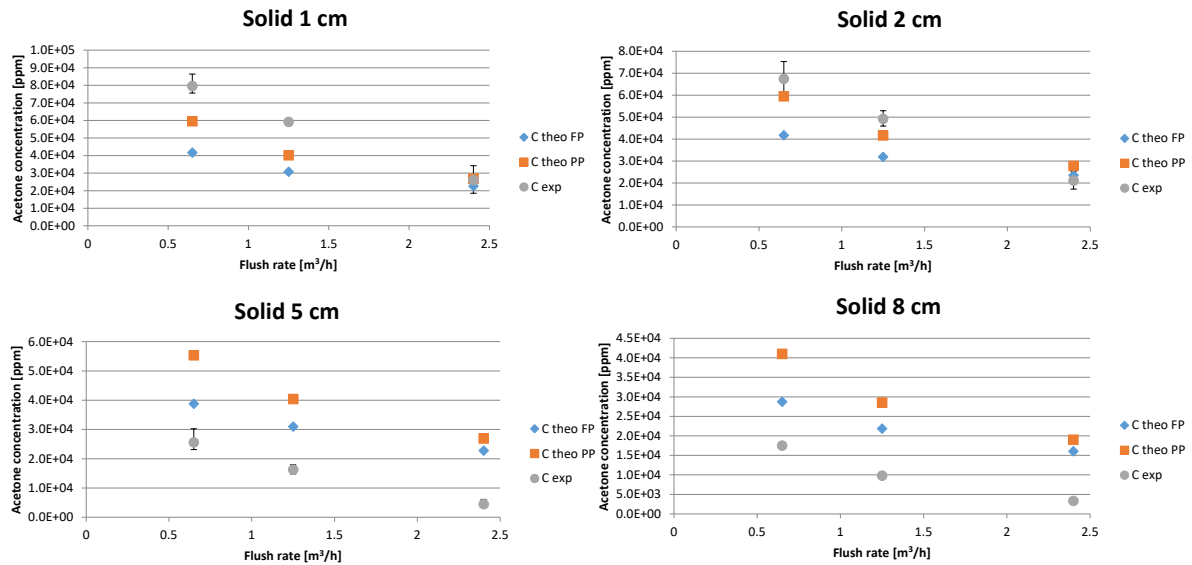
Table 3. *Static concentrations comparison.*

	Cst exp [ppm]	Cst theo [ppm]	T,ace [°C]
1 cm	221000	243000	20
	Cst exp [ppm]	Cst theo [ppm]	T,ace [°C]
2 cm	194000	243000	20
	Cst exp [ppm]	Cst theo [ppm]	T,ace [°C]
5 cm	222000	224000	19.1
	Cst exp [ppm]	Cst theo [ppm]	T,ace [°C]
8 cm	212000	167000	19.5

As previously discussed, the Matlab® code allows to have an idea of the time required for the system to reach the stationary condition, which is the time that should be waited before initiating the fluxed experiments; however, since that time may become very high for higher bed thicknesses, for practical reasons that time was approximated with the time required to

reach a concentration value forthcoming to the stationary value. In Tab. 3, both theoretical ($C_{st\ theo}$) and experimental ($C_{st\ exp}$) concentration static values, are taken at the time chosen to start the flushed tests: 22 min for the 1 cm bed thickness, 30 min for the 2 cm bed thickness, 60 min for the 5 cm bed thickness, 60 min for the 8 cm bed thickness.

Finally, it is possible to evaluate the outlet concentrations as well for the flushed experiments, exploiting Eq. (24), as shown in Fig. 7; in particular, in the application of Eq. (26) the base area A_b was doubled to take account of the greater evaporating surface due to the presence of the microspheres.

Figure 7. *Comparison of theoretical and experimental outlet concentrations.*

Also in this case experimental errors are contained and the errors bars are scarcely visible.
It can be observed, qualitatively, that the forecasted trends agree with the experimental ones. However, there are differences and discrepancies; this may depend on the presence of a capillarity rise as demonstrated by Mauri (2011) who suggests that for the present situation the capillary rise in the solid bed of the liquid can reach up to 2 cm, or from an even higher evaporating surface or both; however further study are necessary. In any case, this is the reason why we considered as significant for the results concerning the solid bed only those relevant to the higher thicknesses, i.e. 8 cm and 5 cm.

Fig. 6 shows that, in presence of the solid, all the resistance is in the solid phase, thus the results do not depend on the fluid dynamics in thewind tunnel, thereby demonstrating that there is no difference between the results obtained with the model of parallel plates (PP) and the model of flat plate (FP).

4. Conclusions

In the present study the problem of the emissions assessment from porous media was addressed. First two models for this purpose were presented (i.e. FP and PP), discussing the features of each option. Experiments were performed with a laboratory scale WT device designed for studies on solid surfaces. The experiments provided significant observations; they confirmed that also for the case of solid sources the outlet concentration and the emission rate depend on flow rate of the neutral air sweeping the surface, even if it is crucial to

properly describe the phenomena taking place inside the solid bed and to correctly define the mass transfer coefficient.

For the flushed period, the analogy with a flow over a flat emissive plate was chosen as the most reliable description of the system.
The theoretical model adopted is the model for mass transfer for the geometry of a flat plate and the regime is laminar with the fluid dynamics boundary layer fully developed and the mass transfer boundary layer not developed.
This model was chosen since it was deemed the one that better describes the studied situation. In facts, for the situation here inspected, where the Schmidt's number is greater than 0.6, the material boundary layer is always comprised inside the fluid dynamics boundary layer that develops until reaching a height equal half of the chamber's grates height (i.e. 2.5 cm). Therefore, for laminar regime with Reynolds' number always lower than 350'000, the mass transfer phenomenon is not affected by the presence of the second plate, i.e. the top wall of the hood, which allows to say that the flat plate analogy is acceptable for the situation of interest, i.e. emissions from porous media. The experimental work allowed to confirm that the chosen model is capable of describing the real situation as the agreement between experimental and calculated values is fairly good. It was also found that the concentration trends in the presence of the solid bed depend only on the fluid dynamics in the solid, which leads to a dependence on (v) more close to -1.

Differences in numerical data are probably due to effective area and capillarity rise; further study will be necessary to better investigate these phenomena. It is worth remarking here once more that, due to the possibility of significant capillary rise, as discussed. The experiments considered to be relevant for the discussion are those referring to the higher bed thicknesses (i.e. 5 cm and 8 cm). However further tests and experiments are required to confirm these findings, modifying the porous medium, the sampling device and/or the investigated compound.

References

Aatamila M., Verkasalo P.K., Korhonen M.J., Suominen A.L., Hirvonen M.R., Viluksela N.K., Nevalainen A., (2011). Odour annoyance and physical symptoms among residents living near waste treatment centres. Environ. Res. 111, 164-170.

Bahlmann E., Ebinghaus R., Ruck W., (2006). Development and application of a laboratory flux measurement system (LFMS) for the investigation of the kinetics of mercury emissions from soils. J. Environ. Manage., 81, 114-125.

Beghi S.P., Rodrigues A.C., De Sa L.M., Santos J.M., (2012). Estimating Hydrogen Sulphide Emissions from an Anaerobic Lagoon. Chem. Eng. Trans., 30, 91-96.

Bird R.B., Stewart W.E., Lightfoot E.N., (2002). Transport Phenomena – Second Edition. W. Anderson and P. Kulek (eds.), John Wiley & Sons Inc., Chapters 6, 14.

Bliss P.J., Jiang K., Schulz T.J., (1995). The Development of a Sampling System for Determining Odor Emission Rates from Areal Surfaces: Part II. Aerodynamic Performance. J. Air Waste Manage. Assoc., 45, 989-994.

Cai L., Koziel J.A., Liang Y., Nguyen A.T., Xin H., (2007). Evaluation of zeolite for control of odorant emissions from simulated poultry manure storage. J. Environ. Qual., 36, 184-193.

Capelli L., Sironi S., Del Rosso R., Céntola P., (2009). Design and validation of a Wind Tunnel system for odour sampling on liquid area sources. Water Sci. Technol., 59, 1611-1620.

Capelli L., Sironi S., Barczak R., Il Grande M., Del Rosso R., (2012). Validation of a method for odor sampling on solid area sources. Water Sci. Technol. 66, 1607-1613.

Capelli L., Sironi S., Del Rosso R., (2013). Odor sampling: techniques and strategies for the estimation of Odor Emission Rates from different source types. Sensors, 13, 938-955.

Catalan L., Liang V., Johnson A., Jia C., O'Connor B., Walton C., (2009). Emissions of reduced sulphur compounds from the surface of primary and secondary wastewater clarifiers at a Kraft Mill. Environ. Monit. Assess., 156, 37-49.

CEN, EN 13725:2003. Air Quality – Determination of Odor Concentration by Dynamic Olfactometry; Brussels, Belgium, 2003.

Dai X.R., Blanes-Vidal V., (2013). Emissions of ammonia, carbon dioxide, and hydrogen sulfide from swine wastewater during and after acidification treatment: Effect of pH, mixing and aeration. J. Environ. Manage., 115, 147-154.

Dunlop M.W., Blackall P.J., Stuetz R.M., (2016). Odour emissions from poultry litter - A review on litter properties, odour formation and odorant emissions from porous materials. J. Environ. Manage., 177, 306-319.

Fingas M. F., (1998). Studies on the evaporation of crude oil and petroleum products II. Boundary layer regulation. J. Hazard. Mater., 57, 41-58.

Frechen F.B., Frey M., Wett M., Löser C., (2004). Aerodynamic performance of a low-speed wind tunnel, Water Sci. Technol. 50, 57-64.

Fricke K., Santen H., Wallmann R., (2005). Comparison of selected aerobic and anaerobic procedures for MSW treatment. Waste Manage., 25, 799-810.

Galvin G., Lowe S., Smith R., (2004). The Validation of a Simple Gaussian Dispersion Model for Determining Odour Emission Rates from Area Sources. Dev. Chem. Eng. Mineral Process., 12, 545-558.

Gostelow P., Parsons S.A., Stuetz R.M., (2001). Odour measurement in sewage treatment – A review. Water Sci. Technol., 35, 579-597.

Guillot J.M., Clincke A.S., Guilleman M., (2014). Odour Emission from Liquid and Solid Area Sources: a Large Intercomparison of Sampling Devices. Chem. Eng. Trans., 40, 151-156.

Guo H., Jacobson L.D., Schmidt D.R., Nicolai R.E., (2003). Evaluation of the influence of atmospheric conditions on odor dispersion from animal production sites. Trans. ASAE, 46, 461-466.

Hayes J.E., Stevenson R.J., Stuetz R.M., (2014). The impact of malodour on communities: a review of assessment techniques. Sci. Total Environ., 500-501, 395-407.

Hudson N. A., Ayoko G. A., (2008). Odour sampling 1: Physical chemistry considerations. Biores. Technol., 99, 3982-3992.

Incropera F.P., DeWitt D.P., Bergman T.L., Lavine A.S., (2007). Fundamentals of Heat and Mass Transfer – Sixth Edition. J. Hayton, V.A. Vargas, S. Rigby, S. Liebman (eds.), John Wiley & Sons Inc., Chapters 6, 7, 8.

Kawamura P. I., MacKay D., (1987). The evaporation of volatile liquids. J. Hazard. Mater., 15, 343-364.

Kolari P., Bäck J., Taipale R., Ruuskanen T.M., Kajos M.K., Rinne J., Kulmala M., Hari P., (2012). Evaluation of accuracy in measurements of VOC emissions with dynamic chamber system. Atmos. Environ, 62, 344-351.

Kozicki W., Tiu C., (1988). A unified model for non-Newtonian flow in packed beds and porous media. Rheol. Acta, 27, 31-38.

Leyris C., Guillot J.M., Fanlo J.L., Pourtier L., (2005). Comparison and development of dynamic flux chambers to determine odorous compound emission rates from area sources. Chemosphere, 59, 415-421.

Loubet B., Cellier P., Flura D., Génermont S., (1999). An evaluation of a wind tunnel technique for estimating ammonia volatilization from land: part 1. Analysis and improvement of accuracy. J. Agr. Eng. Res., 72, 71-81.

Lucernoni F., Tapparo F., Capelli L., Sironi S., (2016). Evaluation of an Odour Emission Factor (OEF) to estimate odour emissions from landfill surfaces. Atmos. Environ. 144, 87-99.

Lucernoni F., Capelli L., Busini V., Sironi S., (2017). A model to relate wind tunnel measurements to open field odorant emissions from liquid area sources. Atmos. Environ. 157, 10-17.

MacKay D., Matsugu R.S., (1973). Evaporation rates of liquid hydrocarbon spills on land and water. Can. J. Chem. Eng., 51, 434-439.

Mauri R., (2011). Fenomeni di Trasporto – Seconda Edizione. R. Mauri (ed.), Edizioni Plus – Pisa University Press, Chapters 4, 14.

Nakano T., Sawamoto T., Morishita T., Inoue G., Hatano R., (2004). A comparison of regression methods for estimating soil-atmosphere diffusion gas fluxes by a closed-chamber technique. Soil Biol. Biochem., 36, 107-113.

Park J.W., Shin H.C., (2001). Surface emission of landfill gas from solid waste landfill. Atmos. Environ., 35, 3445-3451.

Parker D. B., Caraway E. A., Rhoades M.B., Cole N. A., Todd R.W., Casei K. D., (2010) Effect of wind tunnel air velocity on VOC flux from standard solutions and CAFO manure/wastewater. Trans. ASABE. 53 (3), 831-845.

Parker D., Ham J., Woodbury B., Cai L., Spiehs M., Rhoades M., Trabue S., Casey K., Todd R., Cole A. (2013) Standardization of flux chamber and wind tunnel lux measurements for quantifying volatile organic compounds and ammonia emissions from area sources at animal feeding operations. Atmospheric Environment, 66, 72-83

Perry R.H., (1997). Perry's chemical engineers' handbook - Seventh Edition. R.H. Perry, D.W. Green and J.O. Maloney (eds.), The McGraw-Hill Companies, Inc., Chapters 2, 5.

Prata Jr. A.A., Santos J.M., Beghi S.P., Fernandes I.F., Vom Marttens L.L.C., Pereira Neto L.I., Martins R.S., Reis Jr. N.C., Stuetz R.M., (2016). Dynamic flux chamber measurement of hydrogen sulfide emission rate from a quiescent surface - A computational evaluation. Chemosphere, 146, 426-434.

Santos J.M, Kreim V., Guillot J.M, Costa Reis Jr. N., Melo de Sà L., Horan N.J., (2012). An experimental determination of the H_2S overall mass transfer coefficient from quiescent surfaces at wastewater treatment plants. Atmos. Environ., 60, 18-24.

Shah R.K., London A.L. (1978). Laminar flow forced convection in ducts. A source book for Compact Heat Exchanger Analytical Data – First Edition. T.F. Irvine Jr., J.P. Hartnett (eds.), Chapters 1, 6

Sohn J.H., Smith R.J., Hudson N.A., Choi H.L., (2005). Gas sampling efficiencies and aerodynamic characteristics of a laboratory wind tunnel for odour measurement. Bios. Engineer., 92, 37-46.

Song C., Zhang J., Wang Y., Wang Y., Zhao Z., (2008). Emission of CO_2, CH_4 and N_2O from freshwater marsh in northeast of China. J. Environ. Manage., 88, 428-436.

Sutton O.G., (1934). Wind structure and evaporation in a turbulent atmosphere. Proceedings of the Royal Society of London. Series A, Containing papers of a mathematical and physical character, 146, pp. 701-722, London, England, October 1, 1934.

Taha M.P.M., Pollard S.J.T., Sarkar U., Longhurst P., (2005). Estimating fugitive bioaereosol releases from static compost windrows: feasibility of a portable wind tunnel approach. Waste Manage., 25, 445-452.

Thibodeaux L.J., Scott H.D., (1985). Air/Soil exchange coefficients. B. Neely and G.E. Blau (eds.), Environmental Exposure from Chemicals. Vol. I, CRC Press Inc., pp. 65-89.

Thibodeaux L.J., (1996). Chemical exchange between air and soil. J.L. Schnoor and A. Zehnder (eds.), Environmental Chemodynamics: Movement of chemicals in air, water and soil – Second Edition, John Wiley & Sons Inc., Chapter 6, pp. 398-423.

US EPA, (2001). Emissions From Animal Feeding Operations. Draft. U.S. Environmental Protection Agency, Emission Standards Division, Office of Air Quality Planning and Standards, Research Triangle Park (NC), U.S.A.

Van Belois H. J., Anzion C.J.M., (1992). Measurement of emissions over surface areas using the hood method. Stud. Environ. Sci., Biotechniques for Air Pollution Abatement and Odor Control Policies, 439-445.

VDI, (2011). VDI 3880. Olfactometry – Static Sampling, Beuth Verlag GmbH, Berlin, Germany.

Wu B.Z., Feng T.Z., Sree U., Chiu K.H., Lo J.G., (2006). Sampling and analysis of volatile organics emitted from wastewater treatment plant and drain system of an industrial science park. Anal. Chim. Acta, 576, 100-111.

Yellow Book, (1992). Methods for the calculation of physical effects. CPR 14E – Second Edition. Written and reviewed by the Committee for the Prevention of Disasters, Chapter 5.

Zhang H., Lindberg S.E., Barnett M.O, Vette A.F., Gustin M.S., (2002). Dynamic flux chamber measurement of gaseous mercury emission fluxes over soils. Part 1: simulation of gaseous mercury emissions from soils using a two-resistance exchange interface model. Atmos. Environ., 36, 835-846.

Zhang X., Xu M., Liu J., Sun N., Wang B., Wu L., (2016). Greenhouse gas emissions and stocks of soil carbon and nitrogen from a 20-year fertilised wheat-maize intercropping system: A model approach. J. Environ. Manage., 167, 105-114.

Zhang Y., Yue D., Liu J., Lu P., Wang Y., Liu J., Nie Y., (2012). Release of non-methane organic compounds during simulated landfilling of aerobically pretreated municipal solid waste. J. Environ. Manage., 101, 54-58.

Supplementary Material

Appendix A – Chemical Compounds

In the present section, some supplementary material will be presented in order to better explain the performed work.

Here it will be presented a table (Tab. A1) depicting the most common compounds found in the emissions from passive area sources such as: municipal solid waste treatment (MSW), contaminated soils (CS), aerobic waste treatment (AWT), waste water treatment (WWT), animal feeding operations (AFO).

Table A1. Chemical compounds found in emissions from area sources.

Compound	Found in	References	Tb [°C]	Diff in air [cm2/s]	MW [g/mol]	Density [kg/m3]
styrene	MSW	*Zhang et al.* , 2012	145	0.071	104.15	909
benzaldehyde	MSW	*Zhang et al.* , 2012	178	0.073	106.12	1044
toluene	MSW	*Zhang et al.* , 2012	111	0.087	92.14	870
1,2-dichloroethane	MSW	*Zhang et al.* , 2012	84	0.104	98.95	1253
pentane	MSW	*Zhang et al.* , 2012	36.1	0.826	72.15	626
limonene	MSW	*Zhang et al.* , 2012; Perry, 1997	176	0.5111	136.24	841
camphene	MSW	*Zhang et al.* , 2012	159	0.072	136.24	842
alpha-pinene	MSW	Zhang et al., 2012; Perry, 1997	155	0.511	136.24	858
ethanol	MSW	*Zhang et al.* , 2012	78.37	0.115	46.07	789
methylmethacrylate	MSW	*Zhang et al.* , 2012	101	0.077	100.12	940
acetone	MSW, CS, AWT, WWT	*Zhang et al.* , 2012; Fricke et al., 2005; Wu et al., 2006	56	0.124	58.08	791
2-propenal	MSW	*Zhang et al.* , 2012	53	0.105	56.06	839
ammonia	AFO	US EPA, 2001	-33.34	0.259	17.03	730
hydrogen sulphide	WWT	Beghi *et al.* , 2012; Perry, 1997	-60	0.9592	34.08	1.36
mercury	CS	*Zhang et al.* , 2002	356.7	0.031	200.59	13593

Before acetone was adopted as reference compound, experiments were performed also with an aqueous solution of ammonia (NH_3).

Appendix B – Ammonia Experiments

Here results will be presented of experiments involving different compounds and/or different configurations.

For ammonia, the procedure is similar to the one presented for acetone: experiments performed at 3 different flush rates for 3 different thicknesses of the microspheres bed, each run repeated 3 times.

The (averaged) results for the 1 cm thickness of "dry bed" are reported in Tab. B1:

Table B1. *Ammonia concentrations, static and fluxed case, for the 1 cm bed thickness.*

Flux [m3/h]	C exp st [ppm]	C exp fl [ppm]
0.65	136000	50000
1.25	124000	39000
2.4	120000	35000

The (averaged) results for the 2 cm thickness of "dry bed" are reported in Tab. B2:

Table B2. *Ammonia concentrations, static and fluxed case, for the 2 cm bed thickness.*

Flux [m3/h]	C exp st [ppm]	C exp fl [ppm]
0.65	108000	43000
1.25	106000	36000
2.4	104000	34000

The (averaged) results for the 5 cm thickness of "dry bed" are reported in Tab. B3:

Table B3. *Ammonia concentrations, static and fluxed case, for the 5 cm bed thickness.*

Flux [m3/h]	C exp st [ppm]	C exp fl [ppm]
0.65	93000	36000
1.25	90000	33000
2.4	91000	33000

The tables show how the results for higher thicknesses become almost independent on the flush ratio, this is probably due to the high volatility of ammonia and the fact that the emission is controlled more by what happens in the liquid phase. Moreover, another problem encountered was the high variability of the liquid solution – in terms of concentration in the condensed phase - even between one repetition and the next one, an aspect difficultly controllable, which becomes even more severe as temperature increase (i.e. for experiments performed during summertime). These reasons led to the choice of discarding ammonia solutions in favour of a pure compound like acetone that assures no variability of the liquid phase and thus make the emission controlled only by the flush ratio and the bed thickness.

Appendix C – Fluff Layer Experiments

In addition, another possibility was tested, adopting a fluffy layer of material for the bed instead of the glass microspheres.

In this case, instead of the microspheres bed, a fluff material made of nylon was used to simulate the emission source. The results obtained showed a high variability, as depicted below, probably due to the fact that the "solid bed" is very heterogeneous. This led to discard this idea in favour of the glass microspheres bed.

Here in Tab. C1 are reported the static values (i.e. no flux):

Table C1. Acetone concentrations, static case, for the fluff bed experiments.

Flux [m3/h]	t [min]	C exp st [ppm]
0	10	102000
0	30	195000
0	30	217000

Here in Tab. C2 are reported the values obtained for the lower flush rate (i.e. 0.65 L/h):

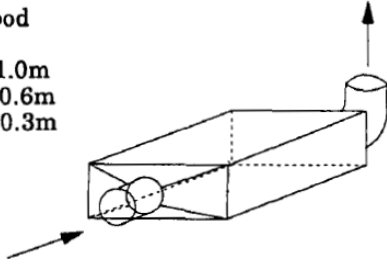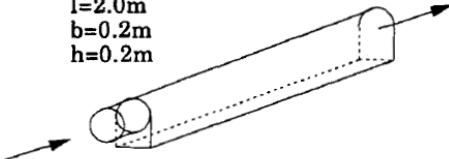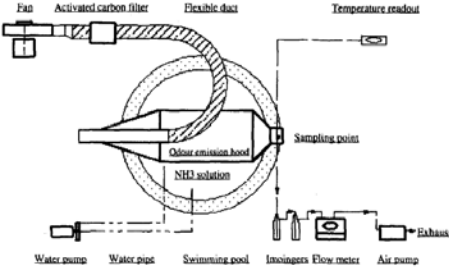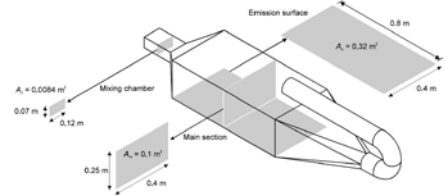*Table C2. Acetone concentrations, flushed case, for the fluff bed experiments.*

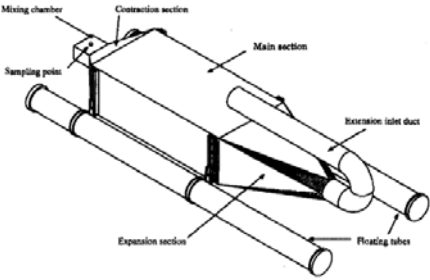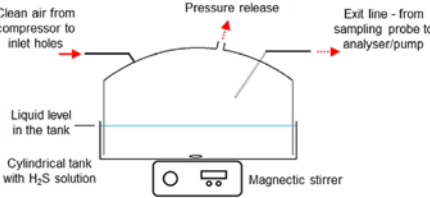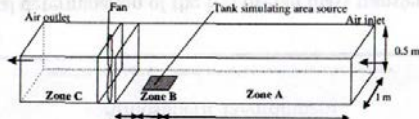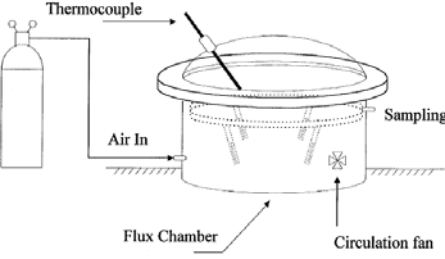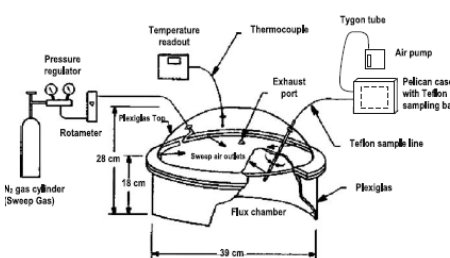| Flux [m3/h]	t [min]	C exp st [ppm]
0.65	3	38000
0.65	6	23000
0.65	2	32000
0.65	2	27000

Appendix D – Dynamic Hoods

Referring to Table 1, in this Appendix it will be presented another table showing an extended overview of possible hoods design, both for Wind Tunnels and for Flux Chambers, as found in the scientific literature.

Table D1. Different kinds of hood design from different authors.

Title and authors	Method of sampling	Design	Parameters	Results

		Air velocity		
Van Belois H. J., Anzion CJ.M. (1992). Measurement of emissions over surface areas using the hood method. Biotechiques for Air Pollution Abatement and Odor Control Policies, 439-445.	Wind tunnel and flux chamber	Hood l=1.0m b=0.6m h=0.3m Wind tunnel l=2.0m b=0.2m h=0.2m	Relationship between <u>air velocity</u> and the measured emission level.	The air velocity in the cover has been varied between 0.1 and 2.2 m/s using an adjustable ventilator. A non-linear relationship was found between the air velocity in the hood or wind tunnel and the emission level, but the value of the exponential proportion was not measured.
Bliss P.J., Jiang K., , Schulz T.J. (1995) The Development of a Sampling System for Determining Odor Emission Rates from Areal Surfaces: Part II. Aerodynamic Performance. Journal of the Air & Waste Management Association, 45:12, 989-994.	Flux chamber	Diameter=1.1 m Height=0.14 m	Relationship between <u>air velocity</u> and the measured emission level.	$$K_c = \frac{0.644 D_A}{L} Re^{1/2} Sc^{1/3}$$ D_A=2.017 x 10^{-5} m^2/s ρ = 1.184 kg/m^3, μ = 1.82 x 10^{-5} kg/(ms), $$K_c = 3.488 * 10^{-3} v^{1/2}$$
Taha M.P.M., Pollard S.J.T., Sarkar U., Longhurst P. (2005). Estimating fugitive bioaereosol releases from static compost windrows: feasibility of a portable wind tunnel approach. Waste Management 25, 445-452.	Wind tunnel		Relationship between <u>air velocity</u> and bioaerosol releases.	$$E_2 = E_1 \left(\frac{v_2}{v_1}\right)^{1/2}$$ E_1= specific bioaerosol emission rate measured using wind tunnel. E_2= specific bioaerosol emission rate corresponding to ground level air velocity. v_1=air velocity inside wind tunnel. v_2=actual ground level air velocity.

Galvin G., Lowe S., Smith R (2004). The Validation of a Simple Gaussian Dispersion Model for Determining Odour Emission Rates from Area Sources. Dev. Chem. Eng. Mineral Process. 12(5/6), pp. 545-558.	Wind tunnel		Relationship between <u>air velocity</u> and emission from solid surfaces.	$E_v = E_1 v_t^{0.63}$ E_v= specific emission rate corresponding to air velocity v. E_1= specific emission rate corresponding to air velocity v equal to 1m/s.
		Liquid boundary layer		
Prata Jr. A.A., Santos J.M., Beghi S.P., FErnandes I.F., Vom Marttens L.L.C., Pereira Neto L.I., Martins R.S., Reis Jr. N.C., Stuetz R.M. (2016). Dynamic flux chamber measurement of hydrogen sulfide emission rate from a quiescent surface - A computational evaluation. Chemosphere 146, 426-434.	Flux chamber	 Diameter = 0.43 m Height= 0.108 m Distilled water =12 L Inlet air flow rate of 5 L/min equally distributed among from four inlet holes. Air temperature = 28.8-35.6 °C Liquid temperature = 29.3-36.5 °C	Effects of <u>fluid flow features</u> on the emission rate measurements. In case of highly volatile compounds, such as H₂S, volatilization is dominated by liquid-phase and the liquid-phase mass transfer conditions (K_L) remain unaffected by the presence of the flux hood. Even if friction velocity at gas-liquid interface is lower (u=6.29*10^-3 m/s) than values normally measured in atmospheric flow, H₂S emission rate obtained numerically and experimentally are similar.	$C_{H_2S} = C_S - (C_S - C_{H_2S_{t=0}})\exp(-t * K_L \frac{A}{V})$ C_S = concentration level at saturation point. $K_L = \frac{1}{k_L} + \frac{1}{Hk_G}$
Santos J.M, Kreim V., Guillot J.M, Costa Reis Jr N.,	Wind tunnel		Volatilization is dominated by <u>liquid-phase</u>,	When concentration in air is negligible:

Melo de Sà L., Horan N.J. (2012). An experimental determination of the H$_2$S overall mass transfer coefficient from quiescent surfaces at wastewater treatment plants. Atmospheric Environment 60, 18-24.			because H$_2$S is a sparingly soluble compound. Environmental parameters that have a significant effect on the overall mass transfer coefficient: - ΔT air-liquid - molecular diffusivity of H$_2$S in water - water density - water viscosity.	$$C_{H_2S} = C_{H_2S_{t=0}} \exp\left(-t * K_L \frac{A}{V}\right)$$ With $$K_L = \frac{1}{k_L} + \frac{1}{Hk_G}$$
		Temperature, Pressure and Humidity		
Park J.W., Shin H.C., (2001). Surface emission of landfill gas from solid waste landfill. Atmospheric Environment 35, 3445-3451.	Flux chamber		Relationship between surface efflux rate, temperature, and pressure.	$$E = \frac{C^*Q}{A}$$ $$E' = E\left(\frac{273}{T+273}\right)\left(\frac{P}{1013}\right)$$ C= concentration [%] Q= incoming air rate to the flux chamber [m^{3}h^{-1}] A=area covered by the flux chamber [m^2] E= specific efflux rate [m^{3}h^{-1}m^{-2}]
Catalan L., Liang V., Johnson A., Jia C., O'Connor B., Walton C. (2009). Emissions of reduced sulphur compounds from the surface of primary and secondary wastewater clarifiers at a Kraft Mill. Environ Monit Assess 156, 37-49.	Flux chamber		Relationship between emissions of reduced sulphur compounds and temperature.	The concentrations of individual reduced sulphur compound at gas-liquid interface are related through Henry's law and Henry's law constant varies with temperature. Results suggest that: - for the primary clarifier only the emission flux of CS$_2$ is significantly correlated with temperature (Pearson's correlation

				coefficient = 0.77) - for the secondary clarifier emission flux of CS_2 (Pearson's coeff=0.40), COS (Pearson's coeff = 0.38) and DMS (Pearson's coeff = 0.40) are significantly correlated with temperature.
Kolari P., Bäck J., Taipale R., Ruuskanen T.M., Kajos M.K., Rinne J., Kulmala M., Hari P. (2012). Evaluation of accuracy in measurements of VOC emissions with dynamic chamber system. Atmospheric Environment 62, 344-351.	Flux chamber		Relationship between emission measurement and <u>temperature and humidity</u>.	- At high relative humidity there is an underestimation of emissions that can be explained by various chemical reactions and physical phenomena taking place on the surfaces of the instrumentations. (An example is formation of thin water film on surfaces) - Chamber effect decreases with raising temperature. In general, emission measurement is most accurate at warm and dry conditions.
		Air flow rate		
Prata Jr. A.A., Santos J.M., Beghi S.P., Fernandes I.F., Vom Marttens L.L.C., Pereira Neto L.I., Martins R.S., Reis Jr. N.C., Stuetz R.M. (2016). Dynamic flux chamber measurement of hydrogen sulfide emission rate from a quiescent surface - A computational evaluation. Chemosphere 146, 426-434.	Flux chamber		Effect of <u>air flow rate</u> on emission measurement.	In case of insufficient air flow there is an artificial increase in compounds concentration in the headspace. This increase reduces the emission rate because the driving force of volatilization decreases. Even when the flow rate is theoretically high, if there is not enough mixing in the air phase, local accumulation can be present.

		Aerodynamic phenomena		
Leyris C., Guillot J.M., Fanlo J.L., Pourtier L. (2005). Comparison and development of dynamic flux chambers to determine odorous compound emission rates from area sources. Chemosphere 59, 415-421.	Flux chamber		Effect of <u>narrowed channels</u> on emission measurement.	The presence of narrowed channels (Top Figure) creates an aerodynamic phenomenon, called unsticking of streamlines, that is unfavorable to convective transfer. For this reason, the measurement of emission rates from the sampled surface is not precise. On the other hand, a chamber without narrowed channels (Bottom Figure) increases the measurement precision because the sampling system does not disturb the natural wind/water surface interaction.